JOURNAL OF MATERIALS SCIENCE 31 (1996) 6129–6135

Cyclic fatigue of a silicon nitride: influence of frequency and fatigue mechanism

Y. H. ZHANG, L. EDWARDS, W. J. PLUMBRIDGE
Fracture Research Group, Materials Department, Open University, Milton Keynes, MK7 6AA, UK

An investigation has been carried out on the slow crack growth behaviour of an advanced Si_3N_4 ceramic material at room temperature at different loading frequencies. The results clearly show a detrimental effect of cyclic loading on crack growth rate in terms of time and a reduced crack growth resistance with increasing cyclic frequency. Crack growth rates can be described by the Paris power-law expression for both static and cyclic loading, but the exponent n increases with decreasing loading frequency. Further support for the existence of mechanical fatigue in this material is provided from experiments involving alternate cyclic and static fatigue using the same specimen, which show substantial differences in crack growth rate in terms of time. Removal of crack wakes resulted in an unchanged crack growth rate under sustained load, which suggests that the crack wake does not play a key role in enhanced crack growth under cyclic loading. The likely crack growth mechanism is discussed.

1. Introduction

Silicon nitrides are candidate materials for heat engine applications due to their high retained strength at elevated temperature, good oxidation resistance and low density. The inherent high sensitivity to microstructural flaws of monolithic silicon nitride can be improved by microstructural modification (for example, by increasing the aspect ratio of grains or by addition of suitable sintering additives) or by incorporating whisker reinforcements, such as SiC. However, adequate knowledge of the mechanical properties of these materials is needed before they can be used in applications requiring structural integrity.

In recent years, the cyclic fatigue behaviour of ceramics has received increasing attention. As in metallic materials, the influence of stress ratio [1, 2], crack size [2, 3], microstructure [4, 5], and environment [6–8] on fatigue life and crack growth rates in ceramics have been increasingly studied. A marked influence of cyclic frequency on fatigue life [9–11] and crack growth rate [12–15] at high temperature has recently been noted. These studies almost unanimously reveal a beneficial effect of cyclic loading at higher frequencies on fatigue lifetime and crack growth resistance at elevated temperature in a variety of materials such as alumina [10], silicon nitride [9, 13, 14] and ceramic composites [12, 14, 16] when compared to sustained loading.

Despite a significant number of investigations on ceramic fatigue at room temperature, the precise mechanism of fatigue crack growth under cyclic loading is still not clear. Three main mechanisms have been postulated:

(i) environmental stress cracking (static fatigue) [17, 18]

(ii) local tensile stresses due to the wedging force around a crack tip created during unloading owing to crack surface roughness [6, 19]

(iii) grain bridging or interlock degradation where the toughening of ceramics by grain bridging is degraded by a wear process during cyclic loading.

Although effects of cyclic frequency on room temperature fatigue life in silicon nitride have been reported in the literature [20, 21], data describing the influence of frequency on crack propagation are limited [6, 22, 23]. Such information is important for fatigue design purposes. Furthermore, the measurement of cyclic fatigue life, or crack growth rate, at different applied frequencies is useful in deciding whether there is true cyclic fatigue in operation, since some workers have suggested that it does not occur in brittle materials such as ceramics [17, 18, 24–26]. Indeed, a recent study has suggested an absence of cyclic fatigue in a monolithic SiC ceramic sample [27]. The present work aims to determine the crack growth characteristics of a silicon nitride sample loaded at different cyclic frequencies, and subsequently to explore the operating crack growth mechanism.

2. Materials and experimental procedures

The material studied is an overpressure sintered silicon nitride containing 7.5 wt % Yttria and 2.5 wt % silica as sintering additives. It was supplied as 54 × 54 × 12 mm tiles by T & N Technology Ltd (Rugby, UK). It has a flexural strength > 500MPa, Weibull moduli > 20 and an average hardness of 1534 Hv at room temperature. The fracture toughness of the

0022–2461

material at room temperature was measured using single-edge-precracked-beam specimens tested under four point bending and found to be 8.7 MPa $m^{1/2}$. The microstructure of the material as revealed by polishing and then etching the surface of a specimen in molten NaOH (at 380 °C) for 1 min is shown in Fig. 1. It consists of elongated grains, which typically have an aspect ratio of over 5:1 and minor diameters of 0.3–2.5 μm.

The tiles were machined into rectangular bars with dimensions $54 \times 10 \times 4.5$ mm. All specimens were ground and then polished to a 3 μm finish. A crack starter was introduced into the top surface of a specimen using a Vickers hardness indentor with an applied load of 20 Kg. The indentation was made at the centre of the polished surface (perpendicular to the pressing direction) of each specimen so that one of the pyramid diagonals was aligned with the longitudinal axis of the specimen. To produce a long through crack from the indent, the bars were precracked using the bridge indentation method [28]. This method basically involves the extension of the crack starter under a decreasing tensile stress field as schematically illustrated in Fig. 2. The crack length can be controlled by the applied load and the selection of anvil span. The typical crack length produced in this study is in the range of 1.0–2.0 mm. Investigation of the effects of initial crack length on crack propagation found that crack growth rates were not dependent on crack length once the crack was over ≈1.0mm in length [29].

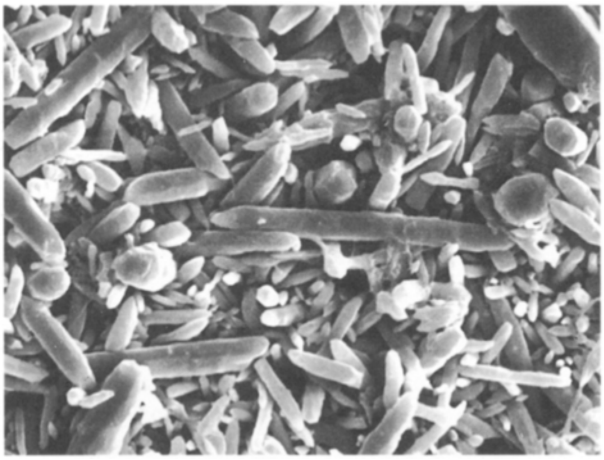

Figure 1 The microstructure of the silicon nitride as revealed by etching in molten NaOH.

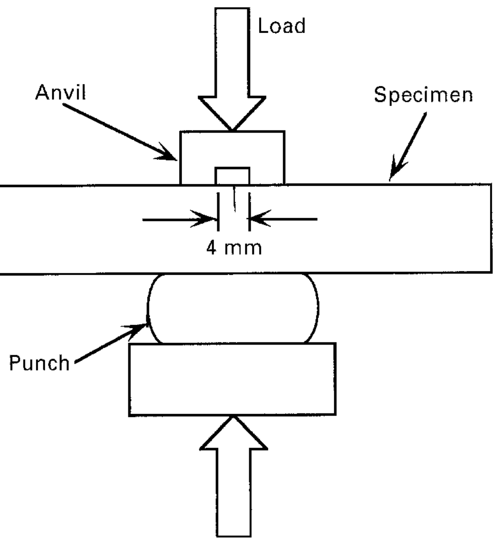

Figure 2 Schematic illustration of the bridge indentation method.

Fatigue tests were performed in a four-point bend fixture with inner and outer spans of 20 and 40 mm, respectively. All fatigue tests were conducted in a high-resolution, computer-controlled electro-servo-hydraulic testing machine (MTS-810 load frame with MTS-458 controller). The crack growth tests were carried out at frequencies of 0.2, 2 and 20 Hz with a stress ratio $R = 0.1$. A sinusoidal waveform was used in all cyclic fatigue tests. At least two specimens were tested at each testing frequency. Static fatigue tests were conducted in the same fixture under sustained load. Initial fast growth from the starter crack was ignored due to the possible influence of residual stress at crack tips produced by bridge indentation.

Crack extension was monitored by interrupting tests after a predetermined number of cycles (or time) and viewing the crack directly on a Reichert MeF3 optical microscope. To measure crack length accurately, a small objective aperture was used to increase contrast and enable the crack tip to be easily located. The crack length, a, was averaged from the measurements on two side surfaces. The crack growth per unit cycle (da/dN) was determined by differentiating the two adjacent data points of crack length versus number of cycles N. This can be expressed as

$$\frac{da}{dN} = \frac{a_i - a_{i-1}}{N_i - N_{i-1}} \tag{1}$$

Stress intensity factors were calculated by means of the following equation [30]:

$$K = FP\beta(\pi a)^{1/2} \tag{2}$$

where

$$\beta = \frac{3(L_2 - L_1)}{2BH^2}$$

and

$$F = 1.122 - 1.40\left(\frac{a}{H}\right) + 7.33\left(\frac{a}{H}\right)^2 - 13.08\left(\frac{a}{H}\right)^3 + 14.0\left(\frac{a}{H}\right)^4$$

and P is the applied load, L_1 and L_2 are the inner and outer span distance, B is the thickness and H is the height of a specimen.

3. Experimental results
3.1 Fatigue crack growth at different frequencies
Crack growth data presented as a function of stress intensity for both constant and cyclic loading with frequencies of 0.2, 2 and 20 Hz are plotted in Fig. 3(a–d). It can be seen that crack growth rates

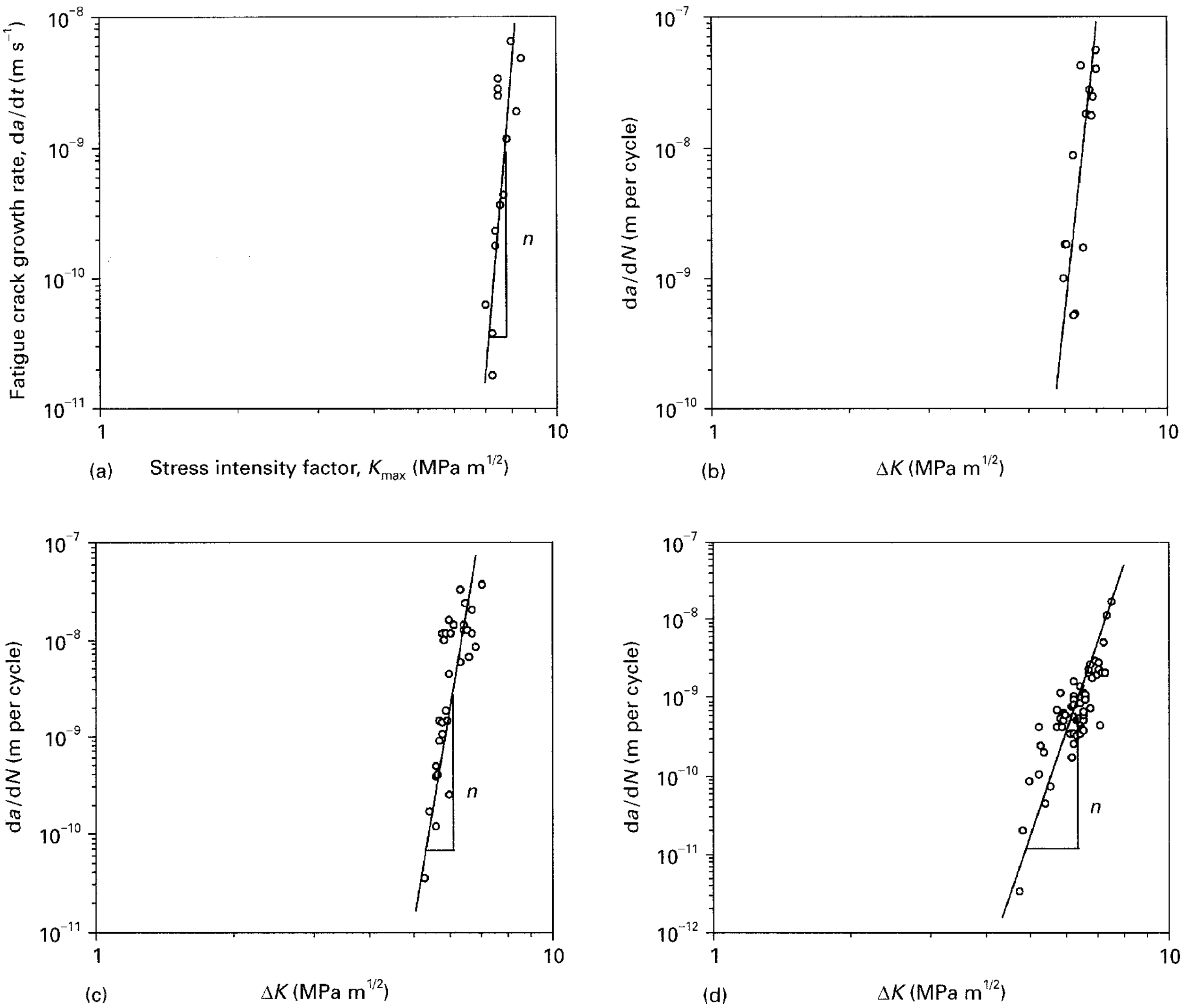

Figure 3 Fatigue crack growth rates versus stress intensity factor at different frequencies. (a) static fatigue; $n = 27$ (b) at a frequency $f = 0.2$ Hz; $n = 23$ (c) at a frequency $f = 2$ Hz and $n = 18$ (d) at frequency $f = 20$ Hz; $n = 11$.

increase with increasing K or ΔK and can be described, as commonly found in fatigue of metallic materials, by the Paris power-law expression:

$$da/dN = A\Delta K^n \quad \text{or} \quad da/dt = BK^n \qquad (3)$$

where A, B and n are usually believed to be material-dependent parameters. However in this case the exponent n is also frequency-dependent. It decreases as the frequency increases. Least squares fitting gives values of n of : $n = 27$ for static fatigue; $n = 23$ at $f = 0.2$ Hz; $n = 18$ at $f = 2$ Hz and $n = 11$ at $f = 20$ Hz.

Fig. 4 compares the crack growth rates versus ΔK at three cyclic frequencies. It can be seen that at high applied ΔK, the crack growth per cycle at lower frequencies ($f = 0.2$ and 2 Hz) is higher than that at higher applied frequency ($f = 20$ Hz). At medium and lower ΔK ranges, the crack growth rates almost coincide. Overall, apart from a minor effect at large ΔK values, the influence of frequency is small.

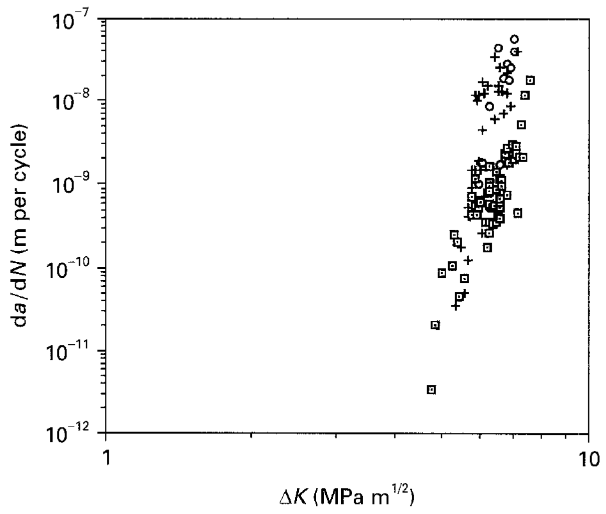

Figure 4 Comparison of crack growth rates, da/dN, at different cyclic frequencies verus ΔK. The frequencies studied were, (⊡) 20 Hz, (+) 2 Hz and (○) 0.2 Hz.

However, when the crack growth rates are expressed as $da/dt(da/dt = (da/dN)f)$ and plotted versus the maximum applied stress intensity factor, $K_{max}(K_{max} = \Delta K/(1 - R))$, as in Fig.5, it can be seen that the crack growth per unit time increases with increasing cyclic frequency with the static crack growth rate the lowest when compared at the same K_{max}. If the cyclic and static fatigue failure mechanisms were both dominated by environmental stress

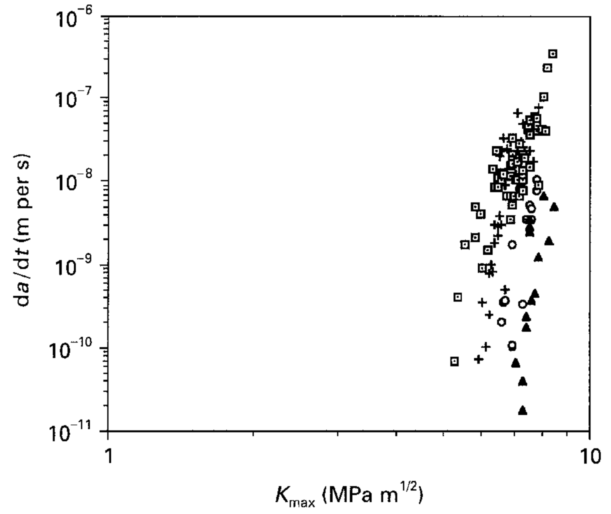

Figure 5 Comparison of crack growth rates, da/dt, at different frequencies versus K_{max}. The frequencies studied were; (▲) static fatigue, (○) $f = 0.2$ Hz, (+) $f = 2$ Hz and (⊡) $f = 20$ Hz.

cracking [17, 18], then the static crack growth rate would be higher than that under cyclic loading because of greater time spent at higher load levels. This is inverse to the present results. Thus, Fig. 5 suggests the existence of true cyclic fatigue in this material.

By comparing the crack growth rates at different frequencies as shown in Figs. 4 and 5, it can be seen that plotting the data against da/dN produces a smaller scatter than da/dt. This suggests that fatigue crack growth of this material is more cycle than time dependent.

3.2 Alternating cyclic and static fatigue

In order to further compare static and cyclic crack growth behaviour and to minimize the masking effect of crack growth rate scatter produced from specimen to specimen, an alternating cyclic and static fatigue test was carried out on a single specimen. After a gradual increase of ΔK at frequency, $f = 20$ Hz, to propagate the bridge indentation induced cracks, the specimens were cyclically loaded at $\Delta K = 6.5$ MPa $m^{1/2}$ with $K_{max} = 7.2$ MPa $m^{1/2}$. After several measurements of crack growth rate at this stress intensity factor range, a static fatigue test was conducted with its stress intensity factor, K_s, identical to the maximum stress intensity factor K_{max} in the previous cyclic loading. Following several further measurements of static fatigue crack growth at this stress intensity factor level, the above procedures were repeated. This is schematically illustrated in Fig. 6. Two specimens were tested in this manner and produced similar results. Fig. 7 shows the result from one of these specimens.

It can be seen that crack growth rates under cyclic loading were in the order of 10^{-7}–10^{-8} m s^{-1} which corresponds to ≈ 30 µm growth in 10 000 cycles (500 s). Once the cyclic load was changed to a sustained load, the crack growth rate quickly dropped to a value $\approx 10^{-10}$–10^{-11} m s^{-1} which is about the same magnitude as those measured in the static-fatigue test shown in Fig. 5. After a total test time of about 26 h,

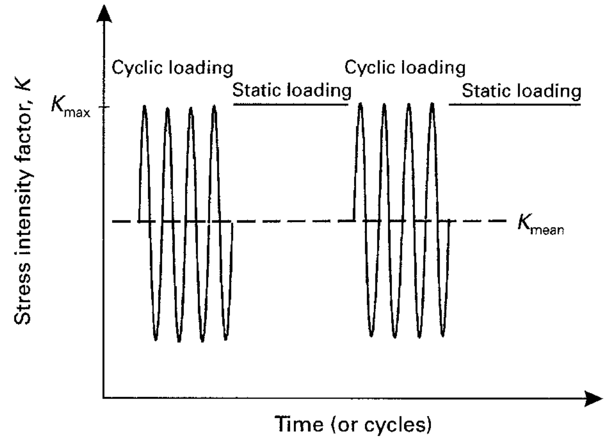

Figure 6 Schematic showing the alternative cyclic and static loading test.

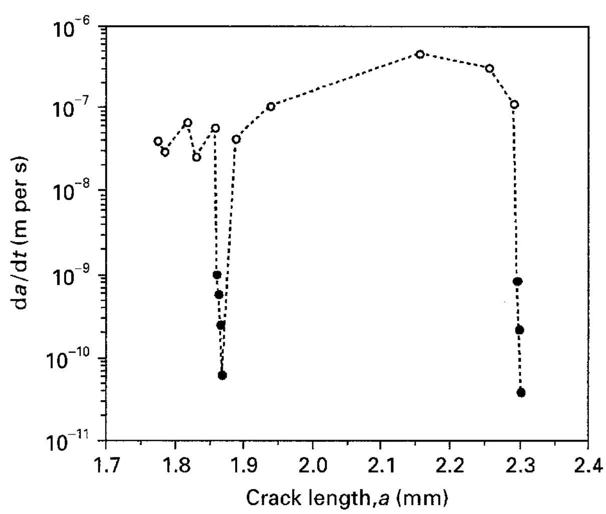

Figure 7 Static loading crack growth rates (open symbols) following cyclic fatigue at $f = 20$ Hz (solid symbols) with K_{max} being constant at 7.2 MPa $m^{1/2}$.

the crack had just grown ≈ 10 µm. Once the cyclic load was applied again, the crack rapidly returned to its original higher level of growth rate. A return to the previous slow crack growth under sustained loading was once more found when the cyclic loading was changed to a static loading. Indeed, to reach approximately the same crack growth rates, the applied stress intensity factor in static fatigue has to be ≈ 1.0 MPa $m^{1/2}$ higher than the K_{max} in cyclic fatigue.

4. Discussion

Since little plastic deformation occurs in brittle materials such as ceramics, it was initially believed that there was no mechanical fatigue in these materials. Early work on fatigue behaviour of ceramics suggested that they only experienced static fatigue in which any subcritical crack growth was attributed to environmental stress cracking [17]. Therefore, the fatigue lifetime under cyclic loading could simply be predicted from static fatigue data on the assumption that cyclic and static fatigue failure mechanisms were identical. The majority of recent evidence supports the existence of cyclic fatigue in ceramics [6, 15, 31]. The possible reason for this apparent contradiction may be that less brittle ceramics, with a higher toughness, have been examined. The susceptibility to cyclic loading of these materials, which usually have microstructural modification, might be different from that of the more brittle ceramics. In silicon nitride, the development of the *in-situ* toughened microstructure greatly increases the fracture toughness of the material causing enhanced resistance to crack propagation.

The present results indicate that only at high applied ΔK is the crack growth rate da/dN affected, with faster growth rates at lower frequencies. This suggests that at high ΔK levels, the increased time spent at load at lower frequencies enhances the crack growth rate which implies time-dependent effects. This fact also suggests that the contribution to crack growth from environment induced cracking is mainly evident when the applied K is comparatively high. This is consistent with the static crack growth result shown in Fig. 3a where the crack growth rate is very sensitive to increase in the stress intensity factor K (high n).

Identifying the precise mechanisms of cyclic crack growth in ceramics is difficult due to the lack of convincing evidence. As the present results and other work indicate environmental stress cracking cannot explain the enhanced crack growth rate under cyclic fatigue and at a higher applied frequency. Progressive degradation of the bridging zone capacity is the main model suggested for this phenomenon [2, 31–36]. In essence, the crack growth driving mechanism in cyclic loading is environmental stress cracking, but the progressive degradation of the bridging force behind the crack tip during cyclic loading leads to less crack tip shielding leading to faster crack growth. The actual stress intensity factor at the crack tip, K_a, in this model can be expressed as:

$$K_a = K_{app} - K_b \quad (5)$$

where K_{app} and K_b are respectively the applied and bridging stress intensity factor. With grain bridge degradation, a gradual decrease of K_b occurs due to the progressive wear of sliding interfaces, leading to a higher crack tip K_a than would occur under static loading conditions compared at the same nominal K, and consequently a faster crack growth rate.

If grain bridging is the main toughening mechanism of crack propagation and cyclic fatigue is primarily caused by the grain bridging degradation, then the rate of growth under static loading will be increased if the crack wake causing grain bridging is removed, i.e., the source of the friction acting against crack opening and closing will be reduced. To investigate this, the crack wake of a specimen which had experienced a cyclic–static–cyclic–static fatigue test was removed using a diamond saw with a blade thickness of 350 μm (Fig. 8). The crack length after the final static fatigue test was 2.225 mm. At first a sawcut of ≈1.5mm long was made. No increase of static crack growth rate was detected in a following static fatigue test for 3 h with the same applied stress intensity factor ($K_s = 7.2$ MPa m$^{1/2}$) as used previously. The crack wake was subsequently removed up to 2.140 mm long giving a remaining sharp crack length of 85 μm. Further static fatigue testing for 16 h under the same K_s produced no increase of crack growth rate, as is shown in Fig. 9. This result implies that the substantially enhanced crack growth rates under cyclic loading observed in this material are not primarily associated with the crack wake and grain bridging degradation.

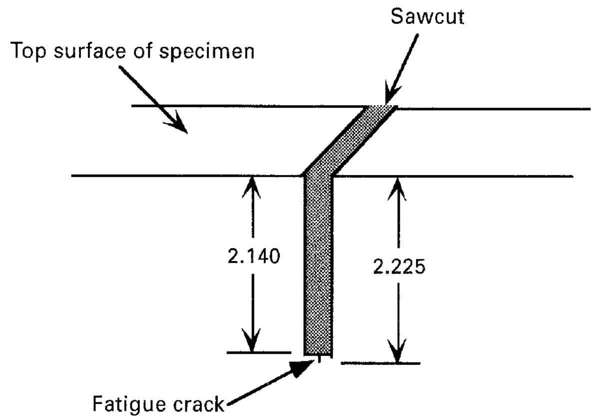

Figure 8 Schematic illustration of crack wake removal.

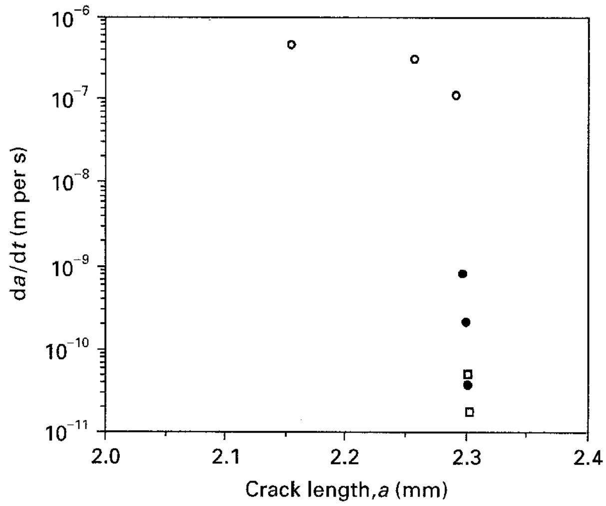

Figure 9 Comparison of crack growth rates before and after crack wake removal. The symbols represent; (○) cyclic fatigue, (●) static fatigue and (□) crack wake removal.

This idea is further supported by our observation of a sudden large drop in da/dt under static fatigue after cyclic loading. If fast crack growth under cyclic loading is indeed caused by grain bridge degradation, then a gradual decrease, or even slight increase, of crack growth rate should be seen when cyclic loading is changed to a constant load. This is because:

(i) the average K value in one cycle was significantly less than the constant K_s(K_{max} in the cyclic fatigue) used in static fatigue

(ii) a grain bridging zone can be extensive. It has been reported that a fully saturated grain bridging zone can reach up to 4.0 mm [34].

However, in the present experiment, a sharp drop of growth rate until almost arrest was observed when a constant load was applied. The previous cyclic loading affected the subsequent static fatigue crack growth rate only for a small crack extension (about 10 μm at $\Delta K = 6.5$ MPa $m^{1/2}$).

In deciding the dominant fatigue crack growth mechanism in ceramic materials it is important to remember that there is likely to be several mechanisms operating and each will have varying degrees of dependence on testing conditions and materials. The present study has revealed two important results:

(i) crack growth rate is basically cycle-dependent

(ii) cyclic fatigue causes limited damage affecting subsequent crack growth rate under static loading.

These suggest that the dominant mechanism of crack growth occurs though a damage zone (or microcrack zone), analogous to the plastic zone in metals, ahead of the crack tip. The comparatively fast crack growth under cyclic loading might be due to the connection of the main crack with the microcracks along grain boundaries within the damaged zone. The concept of a damage zone ahead of a crack tip caused by cyclic loading in ceramics has been previously proposed due to either, (i) a wedging force at the crack wake [6, 19] or (ii) simply by cyclic loading [37, 38].

According to the wedging hypothesis, the crack wake immediately behind the crack tip will be in contact due to debris particles and at asperities during the unloading in the stress cycle. These local compressive contacts generate sufficiently large stresses at the crack tip through a wedging effect to nucleate microcracks along grain-boundaries. The size of these microcracks is then stabilized by the decreasing local stress intensity factor at the crack tip. This wedging effect may well be prominent in an elongated-grain material.

Once the microcracks are formed, some will link up during the rising part of the cycle, causing an enhanced crack growth rate compared to static fatigue. By repeating the above process, a continuous cyclic crack growth can be obtained. Since these microcracks are within a small process zone, which is about a few grain dimensions, the crack growth rate at static load with applied $K_s = K_{max}$ in cyclic load quickly falls to a low value on changing to static loading. In other words, cyclic loading leaves little damage to affect subsequent crack growth at constant loading. This mechanism also explains why cyclic fatigue is absent in materials with a transgranular fracture mode [19], since the wedging effect is directly associated with crack surface asperities due to intergranular crack growth. The faster crack growth rate in terms of da/dN at lower cyclic frequencies is thus caused by the strong contribution from environmental stress corrosion due to the longer time at load. The sharply decreased static crack growth rate following cyclic fatigue test is due to the reduced damage zone size. Under continuous cyclic loading at low frequency with high applied ΔK, however, a small damage zone always exists ahead of the crack front, and the combination of cyclic and static crack growth makes the crack growth faster than that under higher cyclic frequency at the same ΔK level.

5. Conclusions

The principal findings of this investigation are:

(i) Intrinsic cyclic fatigue exists in the silicon nitride ceramic at room temperature and the crack growth resistance deteriorates with increasing cyclic frequency.

(ii) Crack growth rates at all freqeuncies can be described by the Paris power-law expression. The exponent n increases with decreasing applied frequency with static fatigue having the highest value of n.

(iii) Crack growth rates reduce quickly by about three orders of magnitude when a cyclic loading is replaced by a static loading with K_s identical to the previous cyclic K_{max}.

(iv) No recovery of static crack growth rate is found when the crack wake is removed to reduce any possible grain bridging or interlocking.

(v) The experimental results indicate that a grain bridge degradation mechanism is not a major contributor to cyclic fatigue crack growth. It is suggested that enhanced crack growth rate under cyclic loading is due to the continuous production of a microcrack zone and the linkage of these microcracks with the main crack.

(vi) The contribution to crack growth from environmental stress cracking is significant only when cyclic loading causes a damage zone at the crack tip and the applied K is comparatively high.

Acknowledgements

The authors are grateful to the EPSRC and the Open University for support, and to Carol Pindar and John Woodthorpe of T & N Technology Ltd for the provision of materials. They would also like to thank MTS Testing Ltd for their help in developing the testing.

References

1. G. CHOI, S. HORIBE and Y. KAWARE, *Acta Metall. Mater.* **42** (1994) 3837.
2. R. H. DAUSKARDT, M. R. JAMES, J. R. PORTER and R. O. RITCHE, *J. Amer. Ceram. Soc.* **75** (1992) 759.
3. E. Y. LUH, R. H. DAUSKARDT and R. O. RITCHIE, *J. Mater. Sci. Lett* **9** (1990) 719.
4. G. CHOI, S. HORIBE and Y. KAWARE, *Acta Metall. Mater.* **42** (1994) 1407.
5. B. E. CORNELISSEN, R. H. DAUSKARDT, R. O. RITCHIE and G. THOMAS, *ibid.* **42** (1994) 3055.
6. M. OKAZAKI, A. J. MCEVILY and T. TANAKA, *Metall. Trans.* **22A** (1991) 1425.
7. G. CHOI and S. HORIBE, *J. Mater. Sci.* **30** (1995) 1565.
8. S. HORIBE and R. HIRAHARA, *Fatigue Fract. Engng. Mater. Struct.* **14** (1991) 863.
9. T. FETT, G. HIMSOLT and D. MUNZ, *Adv. Ceram. Mater.* **1** (1986) 179.
10. C. K. J. LIN and D. F. SOCIE, *J. Amer. Ceram. Soc.* **74** (1991) 1511.
11. C. K. J. LIN, M. G. JENKINS and M. K. FERBER, *J. Mater. Sci.* **29** (1994) 3517.
12. L. X. HAN and S. SURESH, *J. Amer. Ceram. Soc.* **72** (1989) 1233.
13. S. Y. LIU, I-W. CHEN and T. Y. TIEN, *ibid.* **77** (1994) 137.
14. U. RAMAMURTY, T. HANSSON and S. SURESH, *ibid.* **77** (1994) 2985.
15. L. EWART and S. SURESH, *J. Mater. Sci.* **27** (1992) 5181.

16. U. RAMAMURTY, A. S. KIM and S. SURESH, *J. Amer. Ceram. Soc.* **76** (1993) 1953.
17. A. G. EVANS and E. R. FULLER JR, *Metall. Trans.* **5A** (1974) 27.
18. S. LATHABAI, Y. MAI and B. R. LAWN, *J. Amer. Ceram. Soc.* **72** (1989) 1760.
19. S. HORIBE and R. HIRAHARA, *Acta Metall. Mater.* **39** (1991) 1309.
20. S. F. SHULER, J. W. HOLMES and X. Wu, *J. Amer. Ceram. Soc.* **76** (1993) 2327.
21. T. FETT, D. MUNZ and G. THUN, *J. Mater. Sci. Lett* **12** (1993) 220.
22. K. URASHIMA, Y. TAJIMA and M. WATANABE, in "Cyclic Fatigue in Ceramics", Current Japanese Materials Research Series, Vol.**14**, edited by H. Kishimoto, T. Hoshide and N. Okabe (Elsevier Science B. V. and The Society of Materials Science, Japan, 1995) p. 83.
23. H. KISHIMOTO, A. UENO and H. KAWAMOTO, *ibid.* p. 101.
24. A. G. EVANS, L. R. RUSSEL and D. W. RICHERSON, *Metall. Trans.* **6A** (1975) 707.
25. M. KAWAI, H. FUJITA, Y. KANKI, H. ABE and J. NAKAYAMA, in Proceedings of the First International Symp. on Ceram. Composites for Engines, London, 1983, edited by S. Somiya, E. Kanai and K. Ando (Elsevier, London, 1983) p. 269.
26. S. HORIBE and M. SUMITA, *J. Mater. Sci.* **23** (1988) 3305.
27. R. L. BRETT and P. BOWEN *Int. J. Fatigue* **16** (1994) 559.
28. R. WARREN and B. JOHANNESSON, *Powder Metallurgy* **27** (1984) 25.
29. Y. H. ZHANG and L. EDWARDS, *Scripta Metall. Mater.* **34** (1996) 1561.
30. H. TADA, P. PARIS and G. IRWIN, "The Stress Analysis Handbook", (Del Research Corp., Hellerstown, PA, 1973) p. 213.
31. F. GUIU, M. J. REECE and D. A. J. VAUGHAN, *J. Mater. Sci.* **26** (1991) 3275.
32. S. S. LATHABAI, J. RODEL and B. R. LAWN, *J. Amer. Ceram. Soc.* **74** (1991) 1340.
33. R. H. DAUSKARDT, *J. Engng. Mater. Tech.* **115** (1993) 244.
34. X. Z. HU and Y. W. MAI, *J. Amer. Ceram. Soc.* **75** (1992) 848.
35. F. GUIU, M. Li and M. J. REECE, *ibid.* **75** (1992) 2976.
36. S. OKAWARA, H. KISIMOTO, A. UENO and H. KAWAMOTO, *ibid.* **75** (1992).
37. L. EWART and S. SURESH, *J. Mater. Sci.* **22** (1987) 1173.
38. G. CHOI, *Acta Metall. Mater.* **43** (1995) 1489.

Received 25 March 1996
and accepted 21 May 1996